

HETEROCYCLES, Vol. 106, No. 11, 2023, pp. 1845 - 1854. © 2023 The Japan Institute of Heterocyclic Chemistry
Received, 21st July, 2023, Accepted, 2nd October, 2023, Published online, 17th October, 2023
DOI: 10.3987/COM-23-14888

EFFECTS OF DEGREE OF POLYMERIZATION OF B-TYPE PROCYANIDINS ON AMYLOID AGGREGATION

Taisei Tanaka,^a Hirono Fukushima,^a Vipul V. Betkekar,^b Ken Ohmori,^b
Keisuke Suzuki,^b Yusaku Miyamae,^c and Hideyuki Shigemori^{c,d*}

^aGraduate School of Science and Technology, University of Tsukuba, 1-1-1 Tennodai, Tsukuba, Ibaraki 305-8572, Japan; ^bDepartment of Chemistry, Tokyo Institute of Technology, 2-12-1 O-okayama, Meguroku, Tokyo 152-8551, Japan; ^cInstitute of Life and Environmental Sciences, University of Tsukuba, 1-1-1 Tennodai, Tsukuba, Ibaraki 305-8572, Japan; ^dMicrobiology Research Center for Sustainability (MiCS), University of Tsukuba, 1-1-1 Tennodai, Tsukuba, Ibaraki 305-8572, Japan; E-mail:shigemori.hideyuk.fn@u.tsukuba.ac.jp

Abstract – Amyloid polypeptides are considered to be intensely involved in the pathogenesis of Alzheimer's disease (AD) and type 2 diabetes (T2D), both of which are increasing in incidence worldwide. AD is believed to be caused by the cytotoxicity of amyloid- β (A β) aggregates, while T2D is considered to be due to the cytotoxicity of human islet amyloid polypeptide (hIAPP) aggregates. Therefore, the inhibition of A β and hIAPP aggregate formation can be effective in the prevention of both diseases. Previously, we established that catechol-bearing polyphenolic compounds exhibit remarkable amyloid aggregation inhibitory activities. In this study, we examined the amyloid aggregation inhibitory activities of B-type procyanidins, which have multiple catechol moieties and different degrees of polymerization. We found that all of the tested B-type procyanidins bearing catechol moieties displayed amyloid aggregation inhibitory activity. Furthermore, the higher the degree of polymerization of B-type procyanidins, the stronger the inhibition of amyloid aggregation.

INTRODUCTION

Alzheimer's disease (AD) is the most common neurodegenerative disease worldwide, accounting for 50%–75% of all dementia cases.¹ Type 2 diabetes (T2D) is a disease that causes chronic hyperglycemia due to insulin resistance, insufficient insulin secretion, and various associated complications. An increasing number of reports have shown a link between the two diseases.^{2,3} Both diseases are age-related, and the number of patients is increasing rapidly worldwide owing to the aging population.

Amyloid polypeptides are thought to be closely associated with the pathogenesis of both diseases. Amyloid polypeptides aggregate to form oligomers and fibrils composed of cross β -sheet structures, which have been implicated in various diseases. In particular, amyloid polypeptides, termed amyloid β ($A\beta$), have been implicated in AD, and human islet amyloid polypeptides (hIAPPs) in T2D.⁴ $A\beta$ is a peptide primarily consisting of 40 or 42 residues and it is formed via the cleavage of the amyloid precursor protein (APP), which is involved in synapse formation and repair, by β -secretase (BACE1) and γ -secretase.^{5,6} The accumulation and aggregation of $A\beta$ in the brain causes the atrophy of the hippocampus in the cerebral cortex, which is closely related to learning and memory. In contrast, hIAPP, a peptide consisting of 37 amino acid residues, is produced by islet β -cells and is co-secreted with insulin. hIAPP polymerizes in the vicinity of islet β -cells and forms amyloid aggregates, causing β -cell death and dysfunction.^{7,8} The two amyloid polypeptides have high sequence similarity; they have been reported to aggregate alone as well as co-aggregate.^{9,10}

The accumulation and aggregation of $A\beta$ in the brain has been shown to commence nearly 20 years before symptoms of dementia due to age-related AD appear, and by the time symptoms are observed, the accumulated amount plateaus.¹¹ T2D is a slowly progressing chronic disease that requires long-term treatment. Therefore, it is important to take daily preventative measures against both diseases, and compounds with amyloid aggregation inhibitory activities are considered effective for this purpose. We previously reported that caffeoylquinic acid derivatives, phenylethanoid glycosides, hispidin derivatives, and *p*-terphenyl derivatives inhibit the aggregation of $A\beta_{42}$.¹²⁻¹⁶ In addition, we have shown that kukoamines A and B, schizotenuin A, lycopic acids, rosmarinic acid, clovamide, and A-type procyanidins exhibit inhibitory activity against $A\beta_{42}$ and hIAPP aggregation.¹⁷⁻²² The above-mentioned compounds are catechol-bearing polyphenol compounds, and catechol-type polyphenols are thought to be inhibitors of amyloid aggregation. In this study, we focused on B-type procyanidins, which are polyphenolic compounds with multiple catechol moieties; these procyanidins are abundant in grape seeds. We investigated the effects of synthetic B-type procyanidins comprising catechins different degrees of polymerization on the aggregation of $A\beta_{42}$ and hIAPP. We also examined the differences in the aggregation inhibitory activities of the B-type procyanidins arising from varying degrees of polymerization.

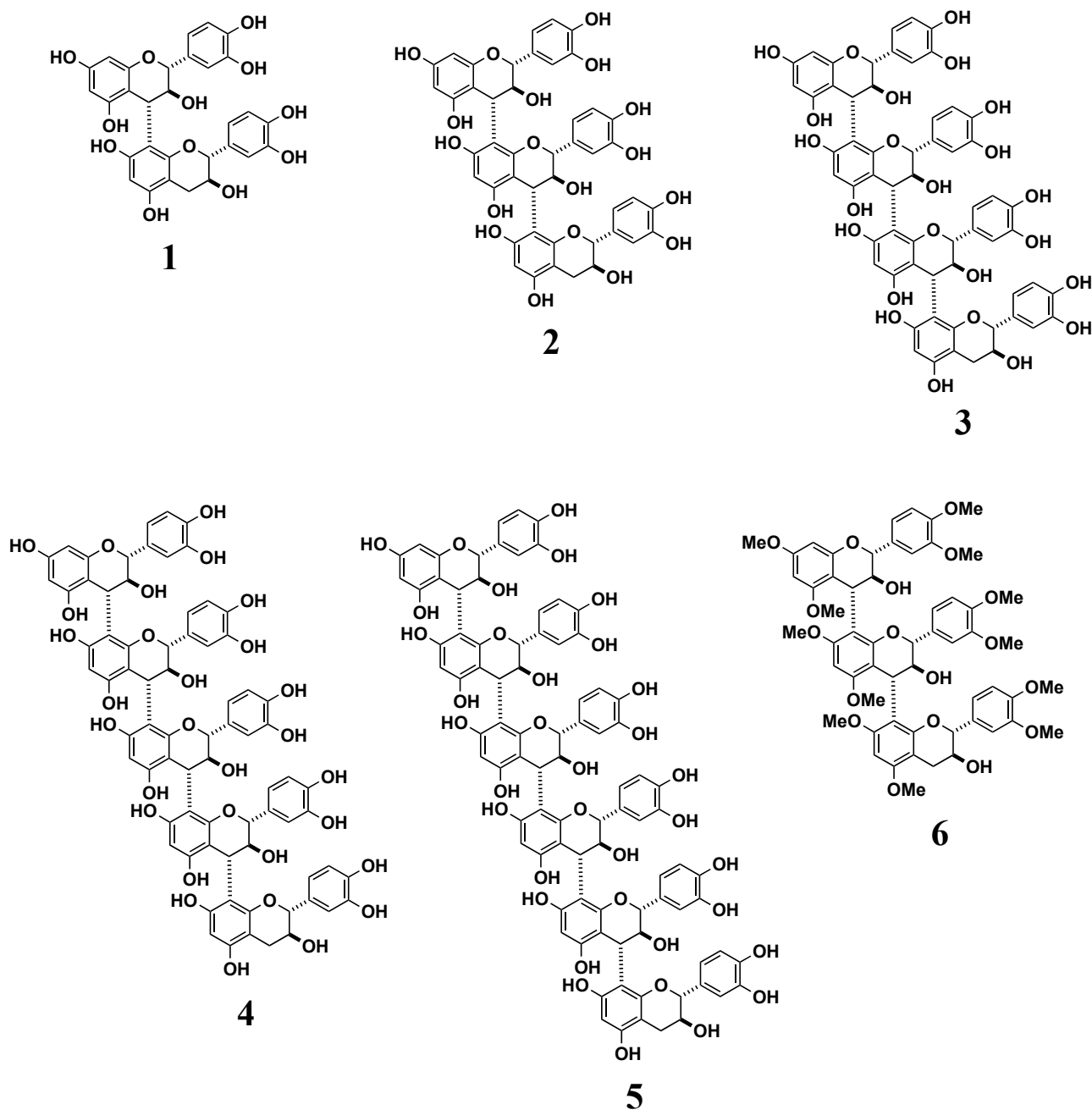


Figure 1. Structures of 1–6

RESULTS AND DISCUSSION

Aggregation inhibitory effects of 1–6 on A β 42

The Thioflavin-T (Th-T) assay was performed to evaluate the inhibitory effects of 1–6 on A β 42 aggregation (Figure 2). When A β 42 was reacted alone, the fluorescence increased with time, reaching a maximum after 4 h and plateauing thereafter. In contrast, the addition of 1–5 suppressed the fluorescence increase over time compared to that observed with A β 42 alone at all concentrations in a concentration-dependent manner. The IC₅₀ values for 1–5 were 34.8, 7.3, 11.3, 3.5, and 4.0 μ M, respectively (Table 1). Compound 1 has already been reported to have moderate A β 42 aggregation

inhibitory activity.²³ The extensively polymerized derivatives, **4** and **5**, showed the highest potency. In contrast, **6**, in which all the phenolic hydroxyl groups were methylated, displayed poor A β 42 aggregation inhibitory activity (>100 μ M).

Transmission electron microscopy (TEM) was performed to examine the effects of **1–6** on the formation of A β 42 aggregates (Figure 3). In the case of A β 42 alone, a large number of interconnected A β 42 aggregates were observed, forming a mesh-like pattern, while a decrease in the amount of A β 42 aggregates was observed in the samples containing **1–5**. However, **6**, which was found not to be active in the Th-T assay, did not induce significant differences in the amount of A β 42 fibers compared to the A β 42-only sample.

The results of the Th-T assay and TEM observations indicate that **1–5** display A β 42 aggregation inhibitory activity, suggesting that the compounds inhibit the formation of β -sheet structures associated with A β 42 aggregation. In general, the A β 42 aggregation inhibitory activity tended to increase as the degree of polymerization of procyanidins increased, with particularly pronounced activity observed for **4** and **5** with higher degrees of polymerization. In contrast, **6**, which does not contain a phenolic hydroxyl group, was found to be inactive. Thus, the importance of the catechol moiety for activity was inferred. The catechol-type flavonoid (+)-taxifolin is thought to inhibit A β 42 aggregation by forming Michael adducts with Lys16 and Lys28 of A β 42 via the *o*-benzoquinone of its B ring.²⁴ Therefore, it is considered that **1–5** inhibit A β 42 aggregation via the same mechanism. The tendency for activity to increase with an increasing degree of polymerization in procyanidins is thought to be due to an increase in the number of catechol moieties, which are the A β 42 reaction sites. The trends observed in the present study support our previous findings regarding the inhibitory effects of CQA, phenylethanoid glycosides, and clovamide on amyloid aggregation.^{12–14,20} However, **2** was slightly more active than **3**, which had an additional catechol structure, suggesting that molecular size and other factors may affect activity.

Table 1. Effects of **1–6** on A β 42 and hIAPP aggregation

Compounds	A β 42, IC ₅₀ (μ M)	hIAPP, IC ₅₀ (μ M)
1	34.8	22.4
2	7.3	7.6
3	11.3	12.7
4	3.5	3.2
5	4.0	2.7
6	>100	>100

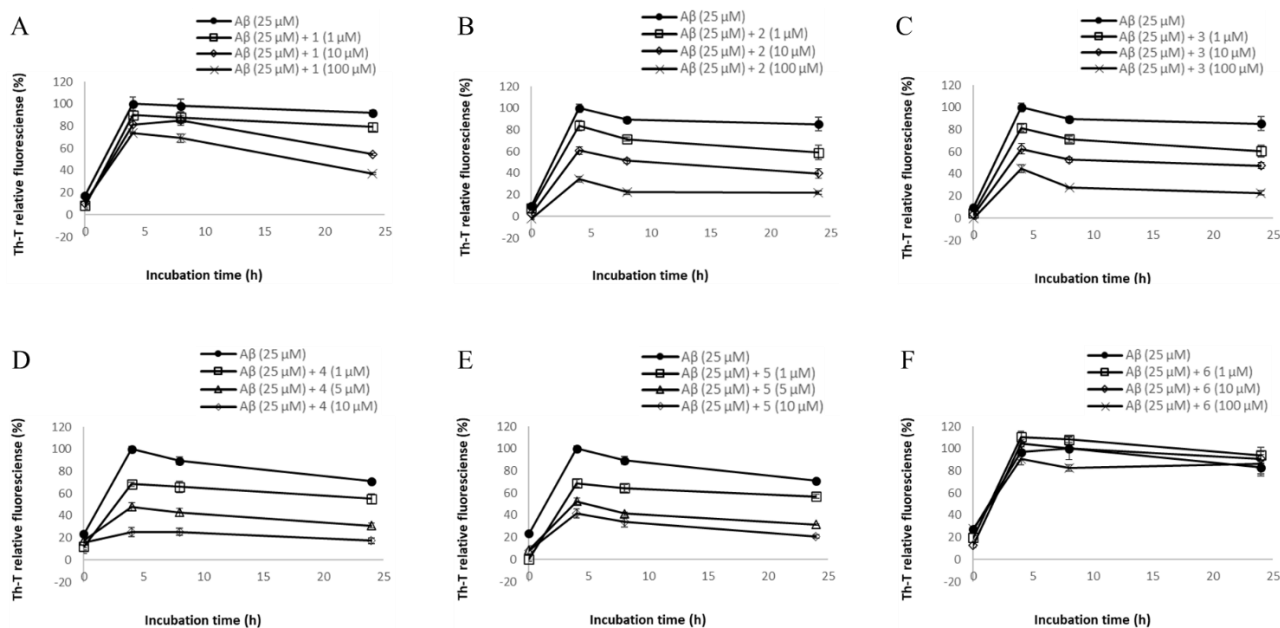


Figure 2. Effects of **1–6** on Aβ42 aggregation. Aggregation of 25 μM Aβ42 was monitored by Th-T fluorescence and observed in the presence the indicated concentrations of **A: 1, B: 2, C: 3, D: 4, E: 5,** and **F: 6**. Fluorescence intensity was measured at an excitation wavelength of 420 nm and emission wavelength of 485 nm, n = 8.

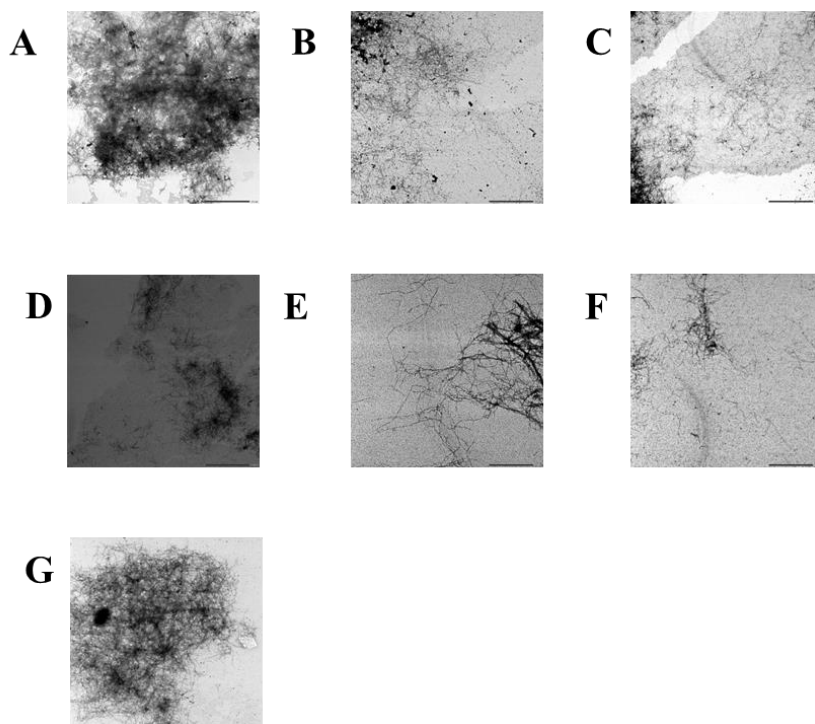


Figure 3. Effects of **1–6** on Aβ42 aggregate formation as observed by transmission electron microscopy (TEM). Scale bars: 2 μm
A: Aβ42 (25 μM), **B:** Aβ42 (25 μM) + **1** (100 μM), **C:** Aβ42 (25 μM) + **2** (100 μM), **D:** Aβ42 (25 μM) + **3** (100 μM), **E:** Aβ42 (25 μM) + **4** (100 μM), **F:** Aβ42 (25 μM) + **5** (100 μM), and **G:** Aβ42 (25 μM) + **6** (100 μM)

Aggregation inhibitory effects of 1–6 on hIAPP

A Th-T assay was performed to evaluate the inhibitory effects of 1–6 on hIAPP aggregation (Figure 4). When hIAPP was reacted alone, the fluorescence increased with time, reaching a maximum after 4 h, and plateauing thereafter. In contrast, the addition of 1–5 suppressed the increase in fluorescence over time compared with hIAPP alone at all concentrations in a concentration-dependent manner. The IC₅₀ values of 1–5 were 22.4, 7.6, 12.7, 3.2, and 2.7 μM, respectively (Table 1). Highly polymerized 4 and 5 showed the highest activities. In contrast, the addition of 6, in which all phenolic hydroxyl groups were methylated, did not inhibit the increase in fluorescence compared to that observed with hIAPP alone. The hIAPP aggregation inhibitory activity of 6 was negligible with an IC₅₀ of >100 μM.

TEM was performed to verify the effects of 1–6 on hIAPP aggregate formation (Figure 5). In the case of hIAPP alone, a large number of interconnected hIAPP aggregates formed a mesh-like pattern, whereas a decrease in the amount of hIAPP aggregates was observed in the presence of 1–5. In contrast, 6, which was not active in the Th-T assay, did not affect the amount of hIAPP fibers compared to the hIAPP-only sample.

The results of the Th-T assay and TEM observations indicated that 1–5 possess hIAPP aggregation inhibitory activity, suggesting that the compounds inhibit the formation of β-sheet structures associated with hIAPP aggregation. In general, the hIAPP aggregation inhibitory activity tended to increase as the degree of polymerization of procyanidins increased, with particularly pronounced activity observed for 4

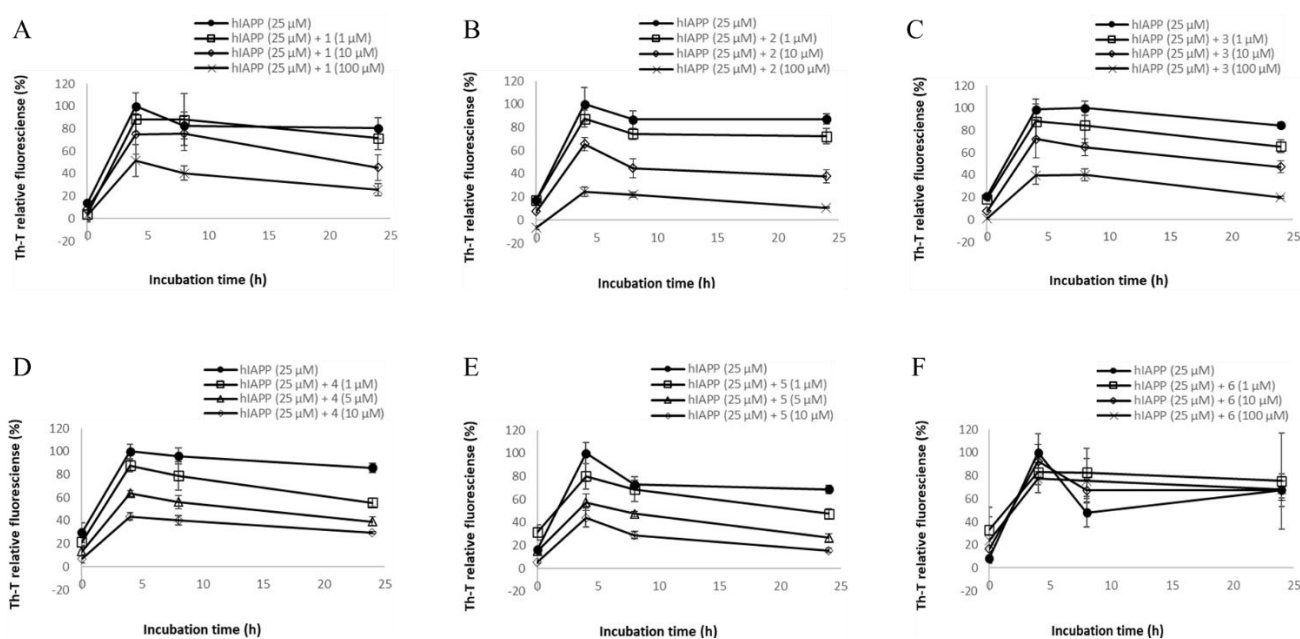


Figure 4. Effects of 1–6 on hIAPP aggregation. Aggregation of 25 μM hIAPP was monitored by Th-T fluorescence and observed in the presence of the indicated concentrations of A: 1, B: 2, C: 3, D: 4, E: 5 and F: 6. Fluorescence intensity was measured at an excitation wavelength of 420 nm and emission wavelength of 485 nm, n = 8.

and **5** with higher degrees of polymerization. In contrast, **6**, which did not contain a phenolic hydroxyl group, was found to be inactive. Thus, a similar trend to that of the A β 42 aggregation inhibitory activity was observed, suggesting the importance of the catechol moiety for activity.

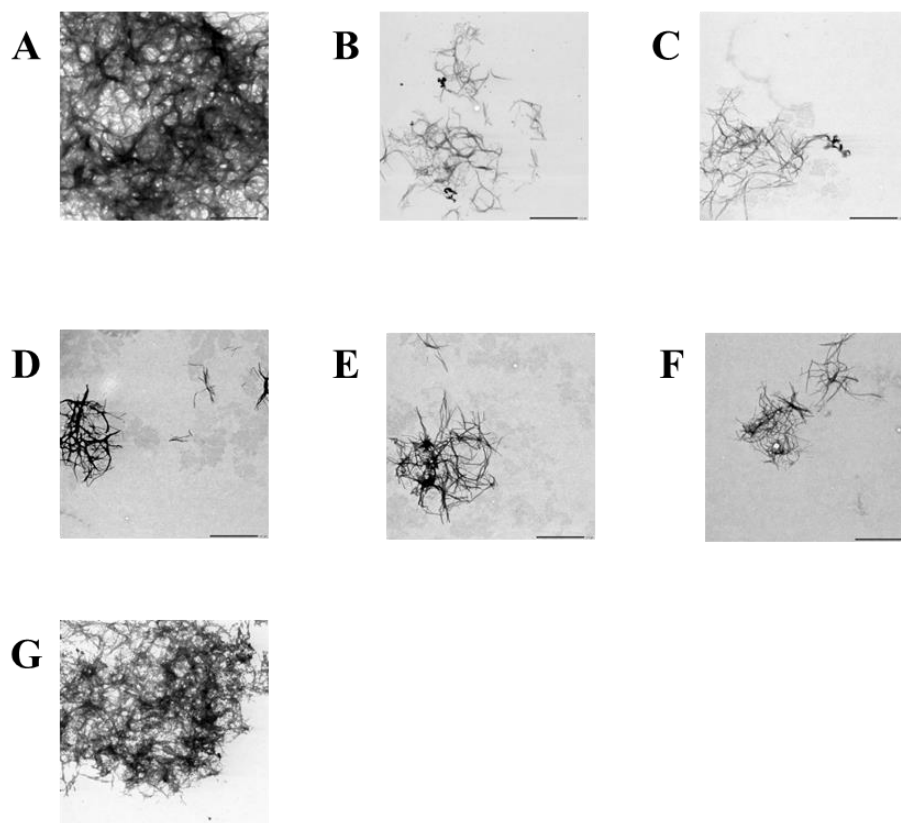


Figure 5. Effects of **1–6** on hIAPP aggregate formation as observed by transmission electron microscopy (TEM). Scale bars: 2 μ m

A: hIAPP (25 μ M), B: hIAPP (25 μ M) + **1** (100 μ M), C: hIAPP (25 μ M) + **2** (100 μ M), D: hIAPP (25 μ M) + **3** (100 μ M), E: hIAPP (25 μ M) + **4** (100 μ M), F: hIAPP (25 μ M) + **5** (100 μ M) and G: hIAPP (25 μ M) + **6** (100 μ M)

CONCLUSION

The aggregation process of A β 42 can be divided into two phases: the nucleation phase, which is thermodynamically less likely to occur, and the elongation phase, entailing fiber elongation. In the nucleation phase, monomeric A β 42 gradually forms low-molecular-weight oligomers, subsequently entering the fiber elongation phase, during which each nucleus acts as a template and binds to a monomer to initiate polymerization.^{25,26} There are three types of aggregation inhibitors: compounds that inhibit nucleation, or elongation, or both. An investigation into which phase of the amyloid aggregation is inhibited by B-type procyanidin should be conducted in the future. Furthermore, it has been reported that amyloid aggregates are more cytotoxic in the oligomeric state than in the full fibrillar state.^{27,28} L-DOPA, which has a catechol structure, inhibits the aggregation of α -synuclein, an amyloid polypeptide

considered to be a causative agent of Parkinson's disease, the major product of which has been shown to be an oligomer.²⁹ It is possible that the compound with the highest activity in the present study also exerts aggregation inhibitory activity by preventing the formation of the highly toxic oligomeric state, constraining the amyloid polypeptide in the fibrillar form, which is less cytotoxic. Therefore, it was necessary to investigate the A β state induced by the presence of the compounds used in this study.

In contrast, it has been reported that hIAPP and the baicalein flavonoid form *o*-benzoquinone and inhibit aggregation as a result of Schiff base formation with Lys1 and Arg11 residues.³⁰ Therefore, it is considered that **1–5** inhibit hIAPP aggregation via the same mechanism. However, **2** was slightly more active than **3**, which had an additional catechol group, suggesting that molecular size and other factors may also influence activity. An investigation into which stage of hIAPP aggregation B-type procyanidins inhibit should be conducted in the future. It is also necessary to investigate the hIAPP state that results in the presence of B-type procyanidins.

Regarding the aggregation inhibitory activity of A β using monomers and oligomers of procyanidins, it has been reported that oligomers are more active.³¹ However, this study is the first to investigate the aggregation inhibitory activity of A β 42 and hIAPP using various purely synthesized procyanidin oligomers.

EXPERIMENTAL

Chemicals

Compounds **1–6** used in this study were synthesized according to a previously published procedure.³² A β 42 was purchased from Peptide Institute Inc., Japan. hIAPP was purchased from KareBay Biochem, Inc. (USA).

Th-T assay

The aggregation of A β 42 and hIAPP was evaluated using the Th-T method developed by Naiki *et al.*³³ The procedure has been described elsewhere.³⁴ Th-T fluorescence assays were performed to evaluate the inhibitory effects of **1–6** on A β 42 and hIAPP aggregation. In brief, A β 42 was dissolved in 0.1% NH₄OH at a concentration of 250 μ M and hIAPP was dissolved in HFIP solution (0.5% acetic acid aqueous solution) at a concentration of 250 μ M. The amyloid polypeptide solution was diluted tenfold with 50 mM PBS (pH = 7.4) and the solution was incubated at 37 °C with or without samples. Both peptides were prepared with 1, 5, 10 μ M or 1, 10, 100 μ M of compounds **1–6** dissolved in PBS. The solution (2.5 μ L) was added to 250 μ L of 5 μ M Th-T in 5 mM Gly–NaOH (pH = 8.5). Fluorescence intensity was measured at an excitation wavelength of 420 nm and emission wavelength of 485 nm using a Wallac 1420 ARVO MX multidetection microplate reader (PerkinElmer). The IC₅₀ value of each compound was calculated from the inhibition rate (%) of amyloid aggregation after 24 h of incubation at 37 °C.

TEM

TEM was conducted to examine the aggregate formation of A β 42 and hIAPP. A total of 5 μ L of the sample of the same composition as the Th-T assay incubated at 37 °C for 24 h was spotted onto a form bar carbon-coated grid that had previously been hydrophilically treated by an HTD-400 hydrophilic treatment system (JEOL), incubated for 2 min, and washed twice with 5 μ L of ultrapure water. Finally, the grid was negatively stained twice for 1 min each with 5 μ L of 0.4% silicotungstic acid, and the solution was removed. After air drying, each sample was examined using a JEM-1400 electron microscope (JEOL).

ACKNOWLEDGEMENTS

TEM observation method was used with JEOL HTD-400 and JEOL JEM-1400 at Center for Medical Electron Microscopy, University of Tsukuba. We would like to thank Editage (www.editage.com) for English language editing. This work was partially supported by JSPS KAKENHI Grant Number JP22H02280.

REFERENCES

1. M. Prince, E. Albanese, M. Guerchet, and M. Prina, *World Alzheimer Report 2014*.
2. J. Janson, T. Laedtke, J. E. Parisi, P. O'Brien, R. C. Petersen, and P. C. Butler, *Diabetes*, 2004, **53**, 474.
3. C. Sims-Robinson, B. Kim, A. Rosko, and E. L. Feldman, *Nat. Rev.*, 2010, **6**, 551.
4. R. Hu, M. Zhang, H. Chen, B. Jiang, and J. Zheng, *ACS Chem. Neurosci.*, 2015, **6**, 1759.
5. G. G. Glenner and C. W. Wong, *Biochem. Biophys. Res. Commun.*, 1984, **120**, 885.
6. C. L. Masters, G. Simms, N. A. Weinman, G. Multhaup, and B. L. McDonald, *Proc. Natl. Acad. Sci. U.S.A.*, 1985, **82**, 4245.
7. J. R. Brender, S. Salamekh, and A. Ramamoorthy, *Acc. Chem. Res.*, 2012, **45**, 454.
8. S. Luca, W. M. Yau, R. Leapman, and R. Tycko, *Biochemistry*, 2007, **46**, 13505.
9. E. Andreetto, L. M. Yan, M. Taterek-Nossol, A. Velkova, R. Frank, and A. Kapurniotu, *Angew. Chem. Int. Ed.*, 2010, **49**, 3081.
10. P. Bharadwaj, T. Solomon, B. R. Sahoo, K. Ignasiak, S. Gaskin, J. Rowles, G. Verdile, M. J. Howard, C. S. Bond, A. Ramamoorthy, R. N. Martins, and P. Newsholme, *Sci. Rep.*, 2020, **10**, 10356.
11. C. R. Jack Jr., D. S. Knopman, W. J. Jagust, R. C. Petersen, M. W. Weiner, P. S. Aisen, L. M. Shaw, P. Vemuri, H. J. Wiste, S. D. Weigand, T. G. Lesnick, V. S. Pankratz, M. C. Donohue, and J. Q. Trojanowski, *Lancet Neurol.*, 2013, **12**, 207.

12. Y. Miyamae, M. Kurisu, K. Murakami, J. Han, H. Isoda, K. Irie, and H. Shigemori, *Bioorg. Med. Chem.*, 2012, **20**, 5844.
13. M. Kurisu, Y. Miyamae, K. Murakami, J. Han, H. Isoda, K. Irie, and H. Shigemori, *Biosci. Biotech. Biochem.*, 2013, **77**, 1329.
14. E. Kidachi, M. Kurisu, Y. Miyamae, M. Hanaki, K. Murakami, K. Irie, and H. Shigemori, *Heterocycles*, 2016, **92**, 1976.
15. Y. Aihara, A. Kawaguchi, M. Hanaki, K. Murakami, K. Irie, and H. Shigemori, *Heterocycles*, 2017, **94**, 1280.
16. A. Kobori, K. Hosaka, and H. Shigemori, *Heterocycles*, 2022, **104**, 925.
17. G. Jiang, M. Takase, Y. Aihara, and H. Shigemori, *J. Nat. Med.*, 2020, **74**, 247.
18. J. Sun, T. Murata, and H. Shigemori, *J. Nat. Med.*, 2020, **74**, 579.
19. J. Sun, G. Jiang, and H. Shigemori, *Nat. Prod. Commun.*, 2019, **14**, 1.
20. T. Tsunoda, M. Takase, and H. Shigemori, *Bioorg. Med. Chem.*, 2018, **26**, 3202.
21. D. Nomoto, T. Tsunoda, and H. Shigemori, *J. Nat. Med.*, 2021, **75**, 299.
22. T. Tanaka, V. V. Betkekar, K. Ohmori, K. Suzuki, and H. Shigemori, *Pharmaceuticals*, 2021, **14**, 1118.
23. M. Mizuno, K. Mori, T. Misawa, T. Takaki, Y. Demizu, M. Shibamura, and K. Fukuhara, *Bioorg. Med. Chem. Lett.*, 2019, **29**, 2659.
24. M. Sato, K. Murakami, M. Uno, Y. Nakagawa, S. Katayama, K. Akagi, Y. Masuda, K. Takegoshi, and K. Irie, *J. Biol. Chem.*, 2013, **288**, 23212.
25. T. R. Serio, A. G. Cashikar, A. S. Kowal, G. J. Sawicki, J. J. Moslehi, L. Serpell, M. F. Arnsdorf, and S. L. Lindquist, *Science*, 2000, **289**, 1317.
26. K. Murakami and K. Irie, *Molecules*, 2019, **24**, 2125.
27. L. Haataja, T. Gurlo, C. J. Huang, and P. C. Butler, *Endocr. Rev.*, 2008, **29**, 303.
28. R. Roychaudhuri, M. Yang, M. M. Hoshi, and D. B. Teplow, *J. Biol. Chem.*, 2009, **284**, 4749.
29. J. Li, M. Zhu, A. B. Manning-Bog, D. A. D. Monte, and A. L. Fink, *FASEB J.*, 2004, **18**, 962.
30. P. Velander, L. Wu, W. K. Ray, R. F. Helm, and B. Xu, *Biochemistry*, 2016, **55**, 4255.
31. E. Y. Hayden, G. Yamin, S. Beroukhim, B. Chen, M. Kibalchenko, L. Jiang, L. Ho, J. Wang, G. M. Pasinetti, and D. B. Teplow, *J. Neurochem.*, 2015, **135**, 416.
32. K. Ohmori, T. Shono, Y. Hatakoshi, T. Yano, and K. Suzuki, *Angew. Chem. Int. Ed.*, 2011, **50**, 4862.
33. H. Naiki and F. Gejyo, *Methods Enzymol.*, 1999, **309**, 305.
34. K. Murakami, K. Irie, A. Morimoto, H. Ohigashi, M. Shindo, M. Nagao, T. Shimizu, and T. Shirasawa, *J. Biol. Chem.*, 2003, **278**, 46179.